*Korean J. Chem. Eng.*, 33(11), 3149-3161 (2016)
DOI: 10.1007/s11814-016-0194-3

pISSN: 0256-1115
eISSN: 1975-7220

# Activated carbon from sewage sludge for removal of sodium diclofenac and nimesulide from aqueous solutions

**Glaydson Simões dos Reis*,**,†, Mohammad Khalid Bin Mahbub**, Michaela Wilhelm**, Eder Claudio Lima***, Carlos Hoffmann Sampaio*, Caroline Saucier***, and Silvio Luis Pereira Dias*****

*Department of Metallurgical Engineering, Federal University of Rio Grande do Sul (UFRGS), Av. Bento Gonçalves 9500, Porto Alegre, RS, Brazil
**University of Bremen, Advanced Ceramics, Am Biologischen Garten 2, IW3, 28359 Bremen, Germany
***Institute of Chemistry, Federal University of Rio Grande do Sul (UFRGS), Av. Bento Gonçalves 9500, Postal Box 15003, ZIP 91501-970, Porto Alegre, RS, Brazil
(*Received 5 February 2016 • accepted 2 July 2016*)

**Abstract**−Sludge based activated carbons (ACs) were used to remove selected pharmaceuticals such as diclofenac (DCF) and nimesulide (NM) from aqueous solutions. The powered sewage sludge was mixed with different proportions of $ZnCl_2$. The mixture was pyrolyzed in a conventional oven using three different temperatures under inert atmosphere. Afterwards, in order to increase the specific surface area and uptake capacity the carbonized materials were acidified with 6 mol $L^{-1}$ HCl under reflux at 80 °C for 3 hours. The characterization of ACs was achieved by scanning electron microscopy, FTIR, TGA, hydrophobicity index by water, n-heptane vapor adsorption and nitrogen adsorption/desorption curves. The specific surface area ($S_{BET}$) of adsorbents varied between 21.2 and 679.3 $m^2g^{-1}$. According to the water and n-heptane analysis data all ACs had hydrophobic surface. Experimental variables such as pH, mass of adsorbent and temperature on the adsorption capacities were studied. The optimum pH, mass of adsorbent and temperature for adsorption of DCF and NM onto ACs were found to be 7.0 (DCF) and 10.0 (NM), 30 mg and 25 °C, respectively. The kinetic adsorption was investigated using general-order, pseudo-first order and pseudo-second order kinetic models, while the general-order model described the adsorption process most suitably. The maximum amounts of DCF and NM adsorbed were 156.7 and 66.4 mg $g^{-1}$ for sample 1(500-15-0.5), respectively.

Keywords: Sewage Sludge, Activated Carbons, Adsorption of Pharmaceuticals, Water and n-Heptane Adsorptions, Adsorption Mechanism

## INTRODUCTION

Pharmaceuticals have caused increasing environmental concerns in recent years as they are a group of ubiquitous, persistent and biologically active compounds with recognized toxicities and endocrine disruption functions. Production and consumption of these products results in pharmaceutical-laden wastewaters [1-3] that must be treated before being discharged into the environment [2,4].

However, conventional wastewater and drinking water treatment processes are not designed to be efficient for removing pharmaceuticals at first instance [5-7]. Consequently, a vast number of these compounds have been detected in effluents of wastewater treatment plants (WWTPs), surface water, ground water, and even drinking water samples [7-9].

Recent studies have shown that several pharmaceuticals are suspected to be directly related to the toxicity of aquatic organisms [9,10]. Continual and undetectable effects, with chronic and accumulative potential, may result in irreversible consequences on wildlife and human beings [10,11]. Therefore, the need for development of an effective method of removing pharmaceuticals from water has become very urgent [12].

Commonly used methods to remove these substances include filtration, ozonization, oxidation, precipitation, coagulation, and adsorption [1,13-17]. However, most of these methods are met with resistance due mainly to the high initial cost involved. In this context, in recent years, many studies have reported the use of the adsorption method for the removal of pharmaceuticals substances in wastewater [1,2,16]. Adsorption is a common, and cost-effective, approach for solving many problems concerning the purification of pharmaceutical-laden wastewaters [1,2,18].

Adsorption is a process by which the pollutants are transferred from the effluent to a solid phase, thereby minimizing the bioavailability of the pollutants to the living organisms [19-21]. Another advantage of the adsorption process is that the adsorbents can be regenerated and reused [20-22].

Among the available adsorbents, activated carbons are known for their excellent adsorption characteristics because of their enhanced pore structures and higher specific surface area. This unique property makes activated carbons one of the materials most used for the treatment of industrial wastewaters [23-25]. The major determinants for the ability of activated carbons to adsorb pollutants from aqueous solutions are the nature of the organic material used to prepare the activated carbon and the experimental conditions of the activation processes [23,25].

†To whom correspondence should be addressed.
E-mail: glaydson.simoes@ufrgs.br, glaydsonambiental@gmail.com

Adsorption using activated carbon has been reported as an effective method of eliminating micropollutants. Saucier et al. [2] showed that pharmaceuticals such as diclofenac and nimesulide were effectively removed by 97 and 98%, respectively, from water using cocoa shell activated carbon with a maximum adsorption capacity of 63.47 and 74.81 mg $g^{-1}$ to DCF and NM, respectively. In contrast, Sotelo et al. [18] reported high uptake values for the micropollutants such as caffeine (190.9 mg $g^{-1}$) and sodium diclofenac (233.9 mg $g^{-1}$) onto commercially available powered activated carbon. Jung et al. [16] showed a higher maximum adsorption capacity value for sodium diclofenac, equal to 372 mg $g^{-1}$ by applying powered activated carbon. The reason for various removal values of micropollutants in the previous researches might be the different experimental conditions used such as the concentration of micropollutants and adsorbent, contact time, pH, and the sample used [2,18,23].

This paper reports the preparation of activated carbons (ACs) from powdered sewage sludge by chemical activation with $ZnCl_2$ using different $ZnCl_2$ : sludge ratios of 0.5, 1.0 and 1.5. The ACs were pyrolyzed at three different conditions under inert atmosphere. Intending to increase the specific area of the ACs, the carbonized materials were acidified with 1.0 mol $L^{-1}$ of HCl to obtain chemically activated sludge based carbons. As far we know, for the first time, ACs prepared from sewage sludge were tested as adsorbents in the removal of pharmaceuticals such as sodium diclofenac (DCF) and nimesulide (NM) from aqueous solutions.

## MATERIALS AND METHODS

### 1. Solutions and Reagents

All solutions were prepared using deionized water. The diclofenac (DCF) and nimesulide (NM) (see Table 1) were supplied by Sigma Aldrich and used without purification. The $ZnCl_2$ was purchased from Vetec and was used for chemical activation of sewage sludge. The characteristics of the pharmaceuticals used on this study are shown in Table 1.

A 1.00 g $L^{-1}$ stock solution of DCF and NM was prepared by weighing and dissolving a calculated amount of the pharmaceuticals in deionized water. Different working solutions were prepared by diluting the stock solution.

### 2. Preparation of Sludge Derived Activated Carbons

The raw material used for preparing the activated carbon was the sewage sludge obtained from a municipal wastewater treatment

**Table 1. Chemical structure of used adsorbates in this study**

| Sodium diclofenac (DFC) | Nimesulide (NM) |
|---|---|
| 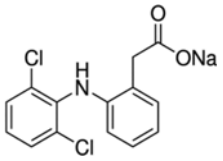 | 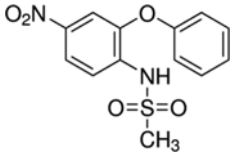 |
| CAS 15307-79-6 | CAS 21803-78-2 |
| $C_{12}H_{10}Cl_2NNaO_2$ | $C_{13}H_{12}N_2O_5S$ |
| 318.13 g·$mol^{-1}$ | 308.31 g·$mol^{-1}$ |
| Log$K_{ow}$=3.91 | Log$K_{ow}$=2.22 |
| pKa=4.00 | pKa=6.70 |
| $\lambda_{max}$=285 nm | $\lambda_{max}$=392 nm |
| Van der Waals surface area=359.64 $A^2$ | Van der Waals surface area=406.46 $A^2$ |
| Polar surface area 52.16 $A^2$ | Polar surface area 104.12 $A^2$ |
| Dipole Moment 19.21 Debye | Dipole Moment 11.52 Debye |
| Polarizability 27.74 | Polarizability 28.28 |

**Table 2. Overview of activated carbons prepared by pyrolysis at different conditions and their respective specific surface areas, pore volume and maximum adsorption values**

| Samples | Pyrol (°C) | Holding time (min) | Ratio $ZnCl_2$/sludge | $S_{BET}$ ($mg^2$ $g^{-1}$) | V ($cm^3$ $g^{-1}$) | $q_{DCF}$ (mg $g^{-1}$) | $q_{NM}$ (mg $g^{-1}$) |
|---|---|---|---|---|---|---|---|
| 1- (500-15-0.5) | 500 | 15 | 0.5 | 679.3 | 0.690 | 162.72 | 63.01 |
| 2- (800-15-0.5) | 800 | 15 | 0.5 | 378.7 | 0.379 | 126.66 | 58.62 |
| 3- (500-60-0.5) | 500 | 60 | 0.5 | 602.5 | 0.493 | 155.48 | 57.31 |
| 4- (800-60-0.5) | 800 | 60 | 0.5 | 405.4 | 0.349 | 142.39 | 55.21 |
| 5- (500-15-1.5) | 500 | 15 | 1.5 | 484.2 | 0.379 | 148.65 | 60.54 |
| 6- (800-15-1.5) | 800 | 15 | 1.5 | 328.0 | 0.422 | 92.69 | 51.35 |
| 7- (500-60-1.5) | 500 | 60 | 1.5 | 662.2 | 0.396 | 151.72 | 49.34 |
| 8- (800-60-1.5) | 800 | 60 | 1.5 | 351.6 | 0.560 | 124.81 | 40.32 |
| 9- (650-37-1.0) | 650 | 37 | 1.0 | 503.7 | 0.422 | 140.32 | 44.35 |
| 10- (500-15-0) | 500 | 15 | 0.0 | 21.2 | 0.007 | 12.33 | 3.88 |

plant in Porto Alegre, RS - Brazil. First, the sludge was dried at 105 °C for 24 h until constant weight loss. Finally, it was crushed with a grinder and sieved to a size range below 300 μm. The preparation of the sludge-based ACs followed the three main steps presented by dos Reis et al. [23]:

a. 10.0 g of powdered sewage sludge was mixed with different amounts of $ZnCl_2$ to adjust different ratios of $ZnCl_2$ : sludge (see Table 2). Subsequently, 5.0 mL of water was added and thoroughly mixed, by hand, to obtain a homogeneous paste. The resulting paste was placed in a crucible and dried at room temperature for 24 h.

b. The samples were pyrolyzed at temperatures and holding times listed in Table 2. The pyrolysis processes were performed using flow of $N_2$ gas with flow rate of 100 mL $min^{-1}$ and at a constant heating rate of 5 °C $min^{-1}$ in a conventional furnace.

c. To complete the chemical activation, a leaching procedure was performed to eliminate the remaining $ZnCl_2$ of the pyrolyzed carbons, and to increase the specific area of the ACs [2,26]. The following procedure was employed [2,26]: 8.0 g of AC were added to 150 mL of 6 mol $L^{-1}$ HCl in a 250 mL reaction flask; the mixture was stirred on a magnetic stirrer under reflux for 3 h at 80 °C. Subsequently, the slurry was cooled and filtered under vacuum using a 0.45 μm membrane in a polycarbonate Sartorius system. After extensive washing with distilled water the solid material was oven dried at 110 °C for 5 h, and finally the carbon sample was milled in a mortar and the activated carbon was sieved to particle sizes ≤90 μm [2,26].

The pyrolyzed materials investigated in this study are listed in Table 2 and are denominated by different numbers. The first number refers to the temperature used in the pyrolysis followed by the holding time and ratio of $ZnCl_2$ : sludge. To give an example, the sample 1(500-15-0.5) was prepared at 500 °C with 15 minutes of holding time and a weight ratio of 0.5/1.0 of $ZnCl_2$ : sludge.

**3. Characterization of the Activated Carbons**

Nitrogen adsorption isotherms were recorded with a commercial system (Belsorp-Mini, Bel Japan Inc.) at −196 °C after drying for 3 h at 120 °C under reduced pressure (<2 mbar). The specific surface areas were determined from the Brunauer, Emmett and Teller (BET) method [27]. The pore size distributions were calculated from the desorption branch of the isotherms based on the Barrett-Joyner-Halenda (BJH) model [28].

Surface morphologies of selected samples were observed by using scanning electron microscopy (SEM) (JEOL microscope, model JSM 6060, Tokyo, Japan).

The functional groups of the adsorbents were assessed using Fourier Transform Infra-Red Spectroscopy (FTIR). The spectrum was recorded with 64 cumulative scans over the range of 4,000-400 $cm^{-1}$ with a resolution of 4 $cm^{-1}$ [29,30].

Thermogravimetric (TGA) analysis of adsorbents were obtained on a TA Instruments model SDT Q600 (New Castle, USA) with a heating rate of 20 °C $min^{-1}$ at 100 mL $min^{-1}$ of synthetic air flow. Temperature was varied from 20 °C to 1,000 °C (acquisition time of 1 point per 5 s) using 10.00-15.00 mg of solid.

For vapor adsorption experiments about 300.0 mg of powder adsorbent was dried in 10 mL beakers at 105 °C for 24 h. The samples were cooled in a desiccator before determining their accurate weight (about 300.0 mg). Storage in an atmosphere of saturated solvent vapor was performed in Erlenmeyer flasks capped with glass caps (45/50 ground glass joint), using 60 ml of solvent (water or n-heptane). The dried powder samples inside the beakers were placed in such a way that they were not in contact with the wall of the Erlenmeyer flasks and kept at 25 °C under static conditions. The beakers containing the solid samples were removed from the Erlenmeyer flasks after 24 h, dried carefully from the outside with laboratory tissues. The weight gain during vapor solvent exposition was used to determine the maximal vapor uptake (of water or n-heptane).

**4. Batch Adsorption Studies**

Aliquots of 20.00 mL of 5.00-500.0 mg $L^{-1}$ of DCF and NM were added to 50 mL flat Falcon tubes containing varying amount of adsorbents (5.0-200.0 mg). The flasks were capped and placed horizontally in a shaker model TE-240, and the system was agitated for time between 5 and 360 min with temperature varying between 25 and 45 °C. Afterwards, in order to separate the adsorbents from the aqueous solutions, the flasks were centrifuged using a Fanem centrifuge, and aliquots of 1-5 ml of the supernatant were properly diluted to 20.0-100.0 ml in calibrated flasks using water [20, 31].

The residual solution after adsorption was quantified using UV/visible spectrophotometer (T90+ UV-VIS spectrophotometer, PG Instruments, London, United Kingdom), at a maximum wavelength of 275 and 392 nm, for DCF and NM, respectively.

The amount of DCF and NM removed by the activated carbons (q in mg $g^{-1}$) and the percentage of removal (%Removal) were calculated with the aid of Eqs. (1) and (2), respectively:

$$q = \frac{(C_o - C_f)}{m} \cdot V \tag{1}$$

$$\%\text{Removal} = 100 \cdot \frac{(C_o - C_f)}{C_o} \tag{2}$$

where q is the amount of DCF and NM uptaken by the absorbent (mg $g^{-1}$); $C_o$ is the initial DCF and NM concentrations put in contact with the adsorbent (mg $L^{-1}$), $C_f$ is the DCF and NM concentrations (mg $L^{-1}$) after the batch adsorption procedure, V is the volume of DCF and NM solutions (L) put in contact with the adsorbent and m is the mass (g) of absorbent.

**5. Quality Assurance and Statistical Evaluation of Models**

All the experiments were in triplicate to ensure reproducibility, reliability and accuracy of the experimental data. The relative standard deviations of all measurements were below 5%. Blanks were run in parallel and corrected when necessary [32].

The solutions of DCF and NM were stored in glass bottles, which were cleaned by immersion in 1.4 mol$L^{-1}$ $HNO_3$ for 24 h [33], rinsing with deionized water, drying and storing them in a suitable cabinet.

Standard solutions of the pharmaceuticals (between 5.00 and 50.0 mg $L^{-1}$) were used for calibration in parallel with a blank solution. A linear analytical calibration curve was performed on the UV-Win software of the T90+PG Instruments spectrophotometer. All the analytical measurements were in triplicate, and the precision of the standards was better than 3% (n=3) [34]. The detection

limit of pharmaceuticals were 0.14 mg $L^{-1}$ with a signal/noise ratio of 3 [35]. A 50.0 mg $L^{-1}$ of standard DCF and NM solutions were used for quality control after every five measurements to ensure accuracy of the pharmaceutical solutions [33].

The mathematical fitness of the kinetic and equilibrium data was done using nonlinear methods, which were evaluated using the Simplex method, and the Levenberg-Marquardt algorithm using the fitting facilities of the Microcal Origin 2015 software. A determination coefficient ($R^2$), an adjusted determination coefficient ($R^2_{adj}$) and the residual standard deviation (SD) were used to evaluate the suitability of the models [21,36]. Residual standard deviation is a measure of the differences between the theoretical and experimental amounts of DCF and NM adsorbed. The $R^2$, $R^2_{adj}$ and *SD* are represented in Eqs. (3), (4) and (5), respectively.

$$R^2 = \left( \frac{\sum_i^n (q_{i,\,exp} - \overline{q}_{i,\,exp})^2 - \sum_i^n (q_{i,\,exp} - q_{i,\,model})^2}{\sum_i^n (q_{i,\,exp} - \overline{q}_{i,\,exp})^2} \right) \tag{3}$$

$$R^2_{adj} = 1 - (1 - R^2) \cdot \left( \frac{n-1}{n-p-1} \right) \tag{4}$$

$$SD = \sqrt{\left( \frac{1}{n-p} \right) \cdot \sum_i^n (q_{i,\,exp} - q_{i,\,model})^2} \tag{5}$$

In these equations, $q_{i,model}$ represents individual theoretical q values predicted by the model; $q_{i,exp}$ represents individual experimental q values; $\overline{q}_{exp}$ is the average of experimental q values; n represents the number of experiments; p represents the number of parameters in the fitting model [21,36].

**6. Kinetic Models**

According to the rate law, exponents of chemical reactions are mostly independent of the coefficients of chemical equations, but are sometimes related. This means that the order of a chemical reaction depends on the experimental data. To establish the general rate law equation for adsorption, the adsorption process on the surface of an adsorbent is considered to be the rate determining step [37,38]. Attention is now focused on the change in the effective number of active sites at the surface of adsorbent during adsorption instead of the concentration of adsorbate in bulk solution. Applying the reaction rate law to Eq. (6) gives the adsorption rate expression.

$$\frac{dq}{dt} = k_N (q_e - q_t)^n \tag{6}$$

where $k_N$ is the rate constant; $q_e$ is the amount of adsorbate adsorbed by adsorbent at equilibrium; $q_t$ is the amount of adsorbate adsorbed by adsorbent at a given time, t; n is the order of adsorption with respect to the effective concentration of the adsorption active sites present on the surface of the adsorbent. Application of the universal rate law to the adsorption process has led to Eq. (6), which can be used without assumptions. Theoretically, the exponent n in Eq. (6) can be an integer or non-integer rational number [37,38].

Eq. (7) describes the number of the active sites ($\theta_t$) available on the surface of adsorbent for adsorption [37,38].

$$\theta_t = 1 - \frac{q_t}{q_e} \tag{7}$$

Eq. (8) describes the relationship between the variable ($\theta_t$) and rates of adsorption.

$$\frac{d\theta_t}{dt} = -k\theta_t^n \tag{8}$$

Where $k = k_N (q_e)^{n-1}$

For an unadsorbed adsorbent $\theta_t$=1, which decreases during the adsorption process. $\theta_t$ approaches a fixed value when the adsorption process reaches equilibrium. For a saturated adsorbent, $\theta_t$=0 [38].

Eq. (8) gives Eq. (9).

$$\int_1^{\theta} \frac{d\theta_t}{\theta_t^n} = -k \int_0^t dt \tag{9}$$

Similarly, Eq. (9) gives Eq. (10).

$$\frac{1}{1-n} \cdot [\theta_t^{1-n} - 1] = -kt \tag{10}$$

Eq. (10) gives Eq. (11) on rearrangement.

$$\theta_t = [1 - k(1-n) \cdot t]^{1/1-n} \tag{11}$$

Substituting Eq. (7) into Eq. (11), and replacing $k = k_N (q_e)^{n-1}$, Eq. (12) is obtained.

$$q_t = q_e - \frac{q_e}{[k_N (q_e)^{n-1} \cdot t \cdot (n-1) + 1]^{1/1-n}} \tag{12}$$

Eq. (12) is the general order kinetic equation of adsorption; valid for $n \neq 1$ [38].

A special case of Eq. (8) is the pseudo-first order kinetic model (n=1) [37,38].

$$\frac{d\theta_t}{dt} = -k \cdot \theta_t^1 \tag{13}$$

Eq. (13) on integration gives Eq. (14).

$$q_t = \exp(-k \cdot t) \tag{14}$$

Substitution of Eq. (7) into Eq. (14), and replacing $k = k_1$ gives the pseudo-first order kinetic model (Eq. (15)).

$$q_t = q_e [1 - \exp(-k_1 \cdot t)] \tag{15}$$

Pseudo-first order kinetic equation is a special case of general kinetic model of adsorption.

When n=2, the pseudo-second-order kinetic model is a special case of Eq. (12) [38].

$$q_t = q_e - \frac{q_e}{[k_2 (q_e) \cdot t + 1]} \tag{16}$$

Eq. (16) on rearrangement gives Eq. (17).

$$q_t = \frac{q_e^2 k_2 t}{[k_2 (q_e) \cdot t + 1]} \tag{17}$$

Pseudo-first-order (Eq. (15)), pseudo-second-order (Eq. (17)), and

general order equation model (Eq. (12)) were used to evaluate the kinetics of adsorption of the pharmaceuticals on the carbon adsorbents.

**7. Equilibrium Models**

In this work, the Langmuir, Freundlich, and Sips [39-41] isotherm models were tested.

The Langmuir isotherm equation is:

$$q_e = \frac{Q_{max} \cdot K_L \cdot C_e}{1 + K_L \cdot C_e} \quad (18)$$

where, $C_e$ is the supernatant concentration after the equilibrium of the system (mg $L^{-1}$), $K_L$ is the Langmuir equilibrium constant (L $mg^{-1}$), and $Q_{max}$ is the maximum adsorption capacity of the material (mg $g^{-1}$) assuming a monolayer of adsorbate uptaken by the adsorbent.

The Freundlich isotherm model is:

$$q = K_F \cdot C_e^{1/n} \quad (19)$$

where $K_F$ the Freundlich equilibrium constant [mg $g^{-1}$(mg $L^{-1}$)$^{-1/n}$] and n is the Freundlich exponent (dimensionless).

The Sips model is an empirical model that consists of the combination of the Langmuir and Freundlich isotherm type models. The Sips [38,41] model takes the following form:

$$q = \frac{Q_{max} \cdot K_S \cdot C_e^{1/n}}{1 + K_S \cdot C_e^{1/n}} \quad (20)$$

where $K_S$ is the Sips equilibrium constant (mg $L^{-1}$)$^{-1/n}$ and $Q_{max}$ is the Sips maximum adsorption capacity (mg $g^{-1}$).

At low adsorbate concentrations the Sips model effectively reduces to a Freundlich isotherm, while at high adsorbate concentrations it predicts a monolayer adsorption capacity characteristic of the Langmuir isotherm.

## RESULTS AND DISCUSSION

**1. Characterization of the Carbon Adsorbents**

Activated carbons were prepared by using sewage sludge as an organic precursor. The chemical activation was carried out using $ZnCl_2$. Ten different activated carbons were pyrolyzed at different temperatures (500°, 650° and 800 °C), using different zinc chloride : organic precursor ratios (0 : 1, 0.5 : 1, 1 : 1, and 1.5 : 1), see Table 2. Afterwards to complete the chemical activation, an acid treatment with 6 mol $L^{-1}$ HCl, under reflux for 2 hours, was used to leach out the inorganic compounds of the carbon structure [26,36]. The ACs were characterized by SEM, elemental analysis, solvent vapor (n-heptane and water) adsorption and $N_2$ adsorption/desorption isotherms. Likewise, the ACs were tested for their performance in the removal of the DCF and NM in aqueous solutions by batch adsorption method. The characterization of activated carbons prepared will be discussed in the following section.

In Table 2 is shown all the textural characteristics of the carbon adsorbents prepared. It was observed that the samples with higher surface area ($S_{BET}$) presented the highest values for adsorption of the anti-inflammatory DCF and NM (see Supplementary Fig. 1). These results show clearly that improvements in the superficial area of the adsorbent are related to increases in the sorption capacity of the adsorbents for DCF and NM [2,26,36].

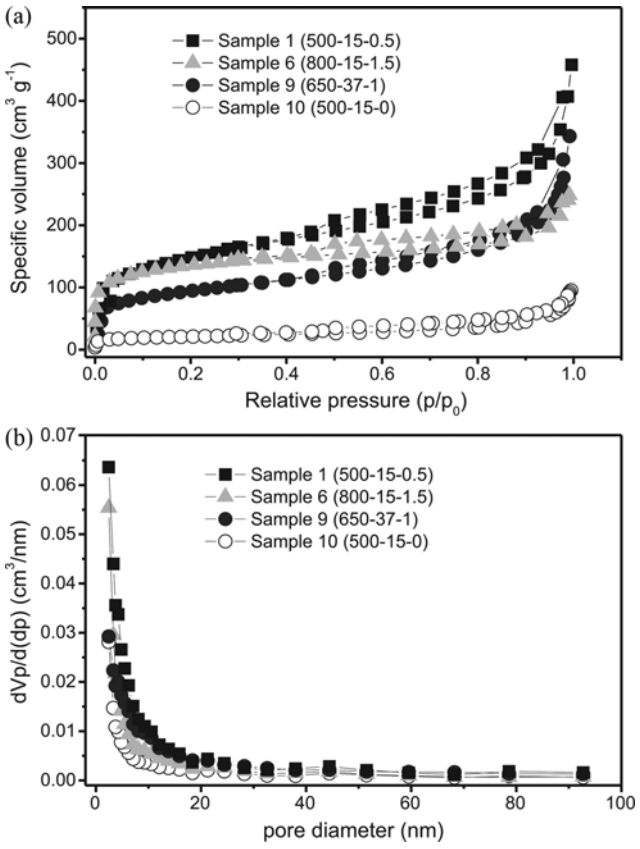


**Fig. 1. (a) Nitrogen adsorption/desorption isotherms for activated carbons and their (b) corresponding BJH plots.**

Samples 1(500-15-0.5) (high surface area), 6(800-15-1.5) (lower surface area), 9(650-37-1.0) (intermediate surface area), and 10(500-15-0) (no chemical impregnation), were chosen to show the effects of chemical activation with $ZnCl_2$ on the evolution of porosity during processing of chemical activation. The isotherms of adsorption and desorption of $N_2$ for other samples are not shown in Table 2 in order to facilitate the visualization of Fig. 1.

All samples can be assigned to be of a type IV isotherm according to the International Union of Pure and Applied Chemistry (IUPAC) classification. Type IV isotherms possess a hysteresis loop with capillary condensation phenomenon indicating mesopores [42]. However, the adsorbed $N_2$ volumes differ in their dependency on the conditions of pyrolysis (Fig. 1(a) and 1(b)). The range of nitrogen volume adsorbed was between 227-458 cm$^3$ g$^{-1}$. Based on Fig. 1(a), it is clear that the sample with higher surface area, sample 1(500-15-0.5), presented higher volume of adsorption when compared with sample 6(800-15-1.5). The lower amount adsorbed can be visualized in sample 10(500-15-0) where no chemical activation was carried out. Based on these results, it is clear that the activated carbons which were obtained by the mixture of sludge with $ZnCl_2$ presented much higher surface area, implying a higher sorption capacity for removal of anti-inflammatories from aqueous solutions, than the sludge without impregnation with $ZnCl_2$.

According to IUPAC classification, micropores have diameters lower than 2 nm, mesopores between 2-50 nm, and macropores

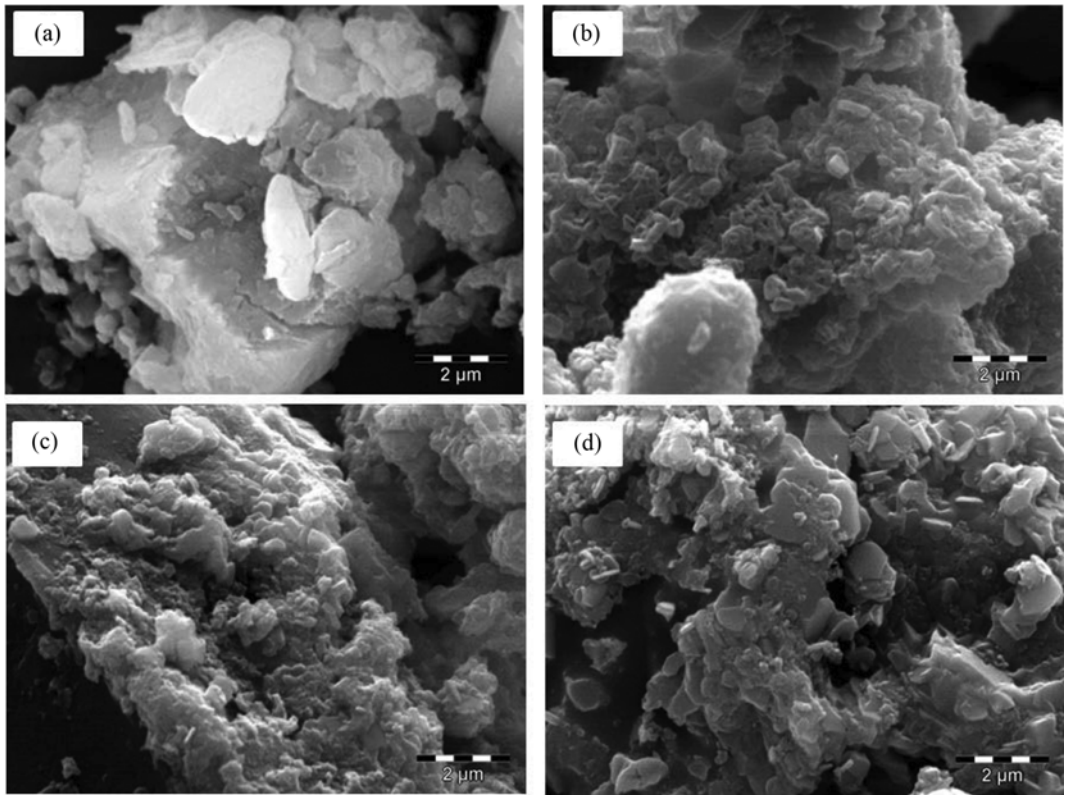


**Fig. 2. SEM images of (a) sample 10(500-15-0); (b) sample 1(500-15-1.5); (c) sample 9(650-37-1.0); and (d) sample 6(800-15-1.5). For description of samples see Table 2.**

higher than 50 nm [42]. All samples possess micropores and mesopores as illustrated in the BJH plots (see Fig. 1(b)).

Structural heterogeneity and internal solid structure can be represented by characterization of the pore size distribution [42]. The pore size distribution visualized by BJH plots of the samples are shown in Fig. 1. By increasing the temperature of production of activated carbon, the samples illustrated a sharp increase in the range of micropores.

The use of a scanning electron microscope (SEM) is one of the most versatile techniques available for the examination and analysis of microstructure morphology characterization, providing detailed surface information such as shape and size of the particles. The SEM images of samples without chemical treatment, sample 10(500-15-0); sample 1(500-15-0.5); sample 9(650-37-1.0); and sample 6(800-15-1.5) are presented in Fig. 2. The roughness of the carbon materials is visible (see Fig. 2). The main difference in roughness concerns the lesser roughness of the non-washed samples compared to the other chemically treated samples that possess higher roughness. This observation could be attributed to the acidic treatments of sample 1(500-15-0.5), sample 9(650-37-1.0) and sample 6(800-15-1.5) that were leached by HCl solution removing practically all the inorganic contents of the samples, as already described in the literature [2,26,36].

The surface polarity of adsorbents is important for interactions with adsorbates that are solutes dissolved in solvents. n-Heptane vapor and water which present different polarities were used to characterize the surface of the adsorbents prepared within this study, as shown in Fig. 3 for all materials. Fig. 3 shows the mass ratio of n-heptane:water uptaken by dried samples of the activated carbons. For all ACs the uptake of n-heptane (which shows mainly dispersive interaction) were higher than the uptake of water (which is mainly polar) demonstrating that the more hydrophobic surfaces of the activated carbons were present in the set of samples [43,44].

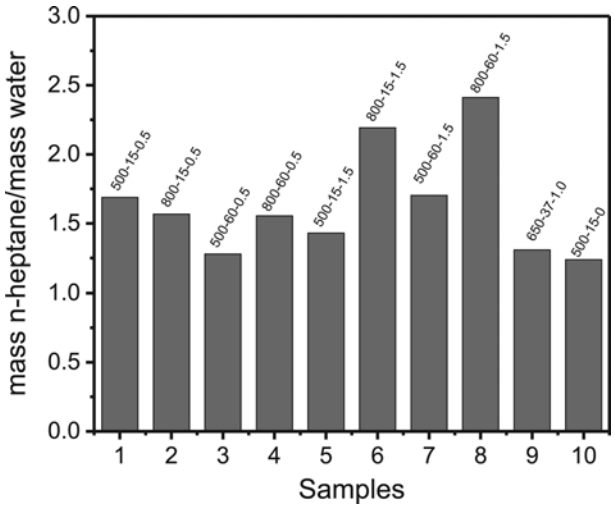


**Fig. 3. Ratio of the maximum sorption capacities of water and *n*-heptane onto activated carbons.**

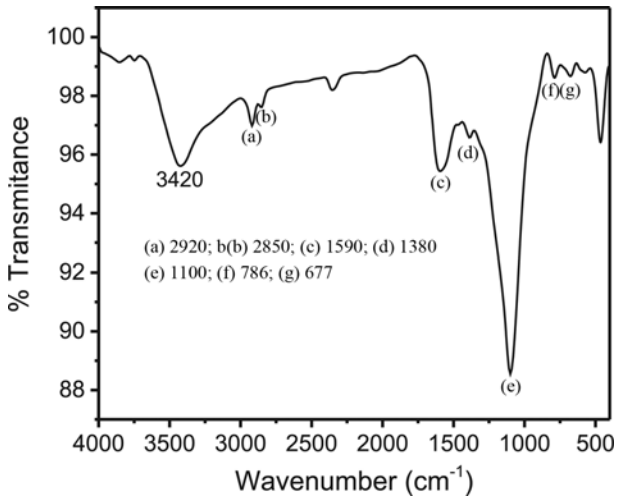


**Fig. 4. FTIR spectra of 1(500-15-0.5) sample activated carbon.**

Samples 6(800-15-1.5) and 8(800-60-1.5) presented higher *n*-heptane : water ratio for the whole set of preparation conditions of ACs. It may be inferred that higher temperature can influence surface characteristics with regards to hydrophobicity. The polarity of the carbon surface should decrease as activation temperature is increased. The unique exception for this observation occurs for sample 2(800-15-0.5), which has practically the same hydrophobic character of the surface of the activated carbon that was obtained for sample 1(500-15-0.5).

The FTIR spectra of the activated carbons revealed that the functional groups present in the carbon adsorbents were almost identical. From which we may infer that the pyrolysis conditions did not have great influence on the rise of different functional groups on the surface among the carbons. Therefore, only the FTIR spectra of the carbon with the highest $S_{BET}$ sample 1(500-15-0.5) are shown and can be seen in Fig. 4. A high-intensity band was observed at 3,420 $cm^{-1}$ which is due to stretching vibrations of the hydroxylic groups [36,37,45,46]. The inconspicuous bands at 2,920 and 2,850 $cm^{-1}$ are ascribed to asymmetric and symmetric C-H stretching [36,37,45,46]. The band at 1,590 $cm^{-1}$ could be assigned to aromatic ring modes [20,24]. The small band at 1,380 $cm^{-1}$ could be assigned to C-H bending vibration [19,20]. The strong absorption at 1,100 $cm^{-1}$ could be assigned to C-O stretching of alcohol and phenol and Si-O of silicates. The small FTIR bands at 786 $cm^{-1}$ are assigned to aromatic out of plane C-H bending; and the bands at 677 $cm^{-1}$ are assigned to aromatic ring bending [19,20].

Therefore, the major groups found in the carbons adsorbents include O-H (alcohols, phenols), aromatic rings, CO (phenols, alcohols), Si-O (silicates), and CH (aromatics, aliphatic).

Fig. 5 shows the thermogravimetric (TG) curves of the 1(500-15-0.5) and 6(800-15-1.5) AC samples. According to the TG curves, the total weight loss of sample 1(500-15-0.5) was 45.97%, and of sample 6(800-15-1.5) was 52.90%. Considering that the atmosphere for performing these experiments of TG was synthetic air, the content left after the thermal treatment of 1,000 °C corresponds to the sample's ash content, as already reported in the literature [2,26,36]. High content of ashes in the samples of adsorbents is directly

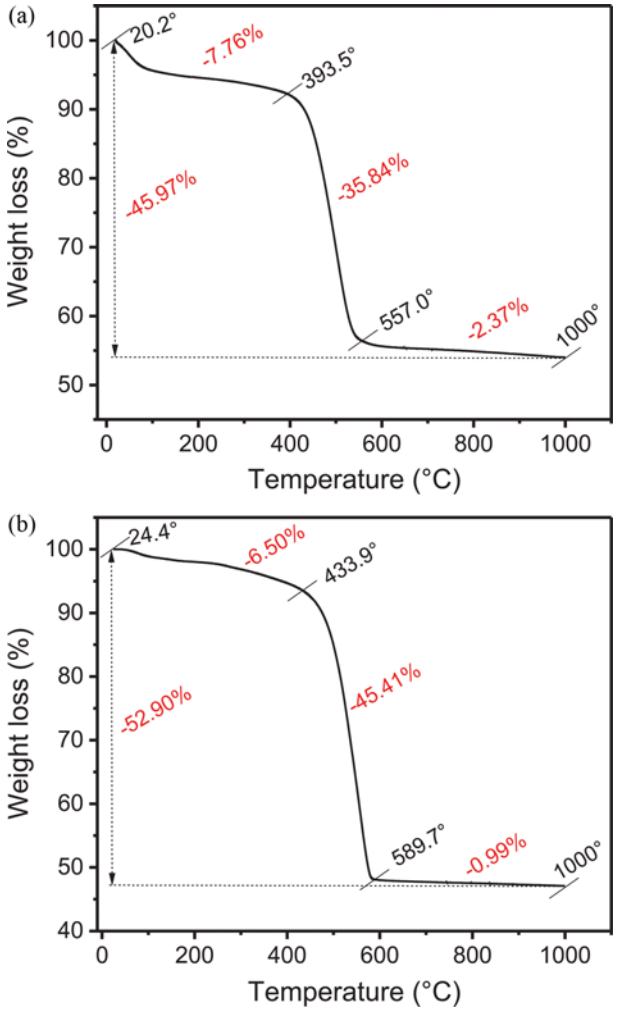


**Fig. 5. TGA and DTG curves of (a) sample 1(500-15-0.5) and (b) sample 6(800-15-1.5).**

related to the sewage sludge used as organic precursor for the production of activated carbon [47,48].

The TG curves can be grouped into three regions of weight loss. The first region ranged from 6.50 to 7.76% (≈20-393.50 °C; for sample 1 from 24.4°-433.9 °C for sample 6, respectively). Such weight loss corresponds to that of adsorbed water, water of crystallization, and water present in the interstitials of the activated carbons [2,26, 36]. Major weight losses occur in the second region. These losses range from 35.84% to 45.41% and from 77.93% to 84.85% for activated carbons. The losses in the second region are attributed to the decomposition of the carbonaceous matrix [26,36,48]. The third stage of weight loss was only 2.37% and 0.99% for sample 1 and 6, respectively. The last stage is attributed to the skeleton decomposition of carbon [36,48] producing ashes, since the atmosphere used in the experiments was synthetic air.

**2. Effects of Initial pH**

One of the most important factors that affect the adsorption process is the pH of the solution [20,21]. Therefore, previous pH studies were carried out to determine which pH would enhance the removal of DCF and NM.

Variations of adsorptions of DCF and NM onto 1(500-15-0.5) sample were investigated in the pH range 6-11 using HCl and/or NaOH to control pH. The effect of pH on DCF and NM removals was studied using 30.0 mg of AC in 20 ml of pharmaceutical solutions (50 mg $L^{-1}$) at an adsorption time of 240 min to make sure that equilibrium was reached. Plots of pH versus removal (%) of DCF and NM at 25 °C are shown in Supplementary Fig. 2.

For DCF, the influence of the pH on the adsorption capacity on AC caused a decrease of the percentage of removal when the pH of solution was increased. On the other hand, for nimesulide, increase of pH of solution increased the amount adsorbed. For instance, at pH 7.0 the percentage removal of DCF was 91.22%, and at pH 11 it decreased to 58.72%. However for NM the percentage removal at pH 7.0 was 72.32%, and at pH 11.0 it was 81.25%, reaching the highest percentage removal at pH 10.0 with 86.94%.

The difference of optimum pH for adsorption of DCF and NM could be explained by the differences of their $pK_a$ values in water. The DCF has a $pK_a$ 4.00 and NM a $pK_a$ 6.70; these values were calculated by the software Marvin Sketch 16.3.14.0. Therefore, at pH 7.0 and 10.0 for DCF and NM, respectively, these pharmaceuticals are deprotonated as anions. Positive groups of surface materials could interact with such anions.

Therefore, on the basis of the above discussion, the optimum pH values for adsorption of DCF and NM onto ACs are pH 7.0 and 10.0, respectively.

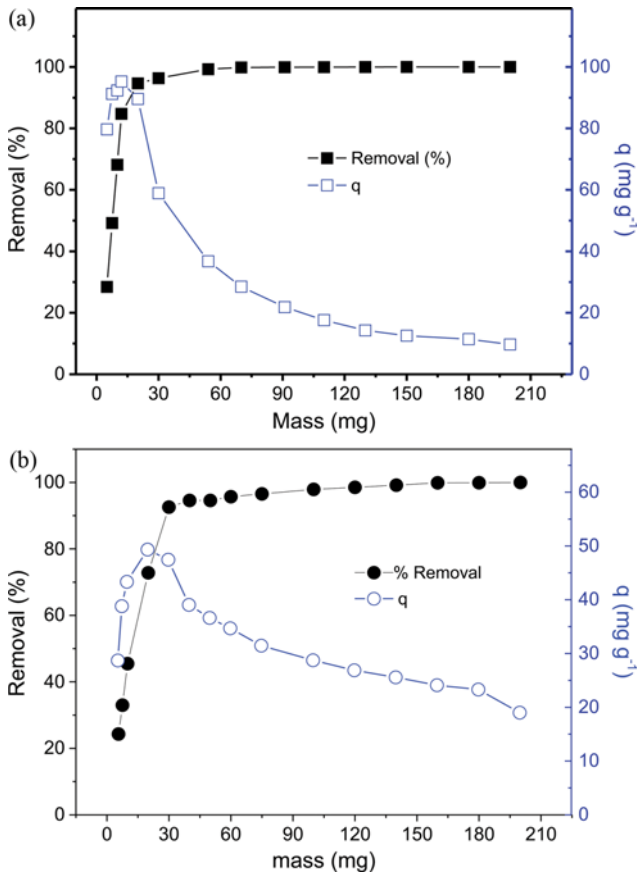


**Fig. 6. Effect of the mass of adsorbent on the % removal and sorption capacity (q) onto sample 1(500-15-0.5).**

### 3. Effect of Adsorbent Mass

The quantity or mass of adsorbent is an important factor in large scale industrial application of adsorbent in the removal of a desired sorbate. The study of adsorbent mass is important in order to avoid waste generation and minimize costs associated with the adsorption process [24,31].

The study of adsorbent dosages for the removal of DCF and NM from aqueous solution was carried out using quantities of 1(500-15-0.5) sludge-activated carbon samples ranging from 5.0 to 150.0 mg with a fixed volume of 20.0 mL of DFC and NM with an initial concentration of 50 mg $L^{-1}$. The optimal adsorption for DCF was attained for a mass of 54.0 mg with 99.24% percentage of removal and q equal to 36.56 mg·$g^{-1}$ (see Fig. 6(a)). However, for the next experiments a mass of 30.0 mg was chosen because at that amount the percentage of removal was 96.34% and q equal to 58.90 mg·$g^{-1}$ (see Fig. 6(a)). This choice is justified because the use of 30 mg instead 54 mg leads an amount reduction of AC in the order of 80% while the decrease of uptake (q) is just 2.91% (see Fig. 6(a)).

A similar trend was observed for NM adsorption, its optimal adsorption was reached at a mass of 60.0 mg with 95.70% percentage of removal and with q equal to 34.68 mg·$g^{-1}$ (see Fig. 6(b)), while a mass of 30.0 mg presented a percentage of removal of 92.56% and a sorption capacity of 47.45 mg $g^{-1}$. Therefore, an increase of 50% of the mass of the adsorbent led to an increase of only 3.14% of removal and a decrease of 26.91% on the sorption capacity. Therefore, the best mass for adsorption experiments was found to be 30.0 mg for each adsorbent.

### 4. Kinetic Studies

To investigate the mechanism of adsorption and potential rate-controlling steps such as chemical adsorption, diffusion control and mass transport processes, kinetic models have been used to test experimental data. These studies give valuable information for adsorption process design, operation control, and evaluation of the adsorbents [1,2,20,21].

Nonlinear pseudo-first order, pseudo-second order and general-order kinetic models were used to assess the kinetics of adsorption of DCF and NM onto the activated carbon that presented the higher surface area, sample 1(500-15-0.5). All other samples presented the same trend for the kinetic studies and sample 1(500-15-0.5) was chosen to demonstrate the parameters of the kinetic models, because it was considered the best adsorbent in this study as it presented highest $S_{BET}$ and performance in uptake of the DCF and NM in aqueous solutions.

Table 3 and Supplementary Fig. 3 show the parameters and curves, respectively, of kinetic experiments performed to determine the equilibrium time required for the uptake of DCF and NM by sample 1(500-15-0.5). The parameters of the curves were obtained by plotting the DCF and NM uptake capacity versus time at 70 mg $L^{-1}$ initial concentration. Adsorption studies were carried out for periods of times between 5 min and 10 hours.

Using the SD and the $R^2_{adj}$ it can be concluded that the kinetic data were best fitted by the general order kinetic model, as already reported in the literature for several adsorbents and adsorbates [1,2,20,21,26,36,37,44,45].

The general-order kinetic model states that the order of an ad-

**Table 3. Kinetic parameters of DCF and NM adsorption onto sample 1(500-15-05) conditions: Temperature, 25 °C; pH 7.0 and 10.0 for DCF and NM, respectively; and mass of adsorbent 30.0 mg, initial anti-inflammatory concentration 70.0 mg $L^{-1}$. All values of the parameters are expressed with four significant digits**

| | DCF | NM |
|---|---|---|
| **Pseudo first-order** | | |
| $k_1$ ($h^{-1}$) | 35.49 | 10.10 |
| $q_e$ (mg $g^{-1}$) | 112.2 | 50.14 |
| $t_{1/2}$ (h) | 0.01953 | 0.06859 |
| $R^2_{adj}$ | 0.9953 | 0.9246 |
| SD (mg $g^{-1}$) | 1.920 | 3.608 |
| **Pseudo second-order** | | |
| $k_2$ (g $mg^{-1}$ $h^{-1}$) | 1.316 | 0.3586 |
| $q_e$ (mg $g^{-1}$) | 113.5 | 52.70 |
| $t_{1/2}$ (h) | 0.006694 | 0.05292 |
| $R^2_{adj}$ | 0.9989 | 0.9829 |
| SD (mg $g^{-1}$) | 0.9093 | 1.716 |
| **General order** | | |
| $K_n$ [$h^{-1}\cdot(g\ mg^{-1})^{n-1}$] | 0.03746 | 0.02893 |
| $q_e$ (mg $g^{-1}$) | 115.5 | 54.97 |
| n | 3.223 | 2.734 |
| $t_{1/2}$ (h) | 0.001144 | 0.04441 |
| $t_{0.95}$ (h) | 0.2431 | 3.249 |
| $R^2_{adj}$ | 0.9997 | 0.9867 |
| SD (mg $g^{-1}$) | 0.5056 | 1.514 |

sorption process should logically follow the same trend as that of a chemical reaction, where the order of reaction is experimentally measured instead of being restrained by a given model [2,38].

Considering that it is difficult to compare the parameters of the general-order kinetic model, since the exponent n is different for DCF and NM, we used $t_{1/2}$ and $t_{0.95}$ to compare the kinetics of DCF and NM. The $t_{1/2}$, that is defined as the time to achieve half of saturation ($q_e$) in the kinetic results, $t_{0.95}$ is the time to achieve 95% of saturation ($q_e$). The $t_{0.95}$ was taken mostly for purposes of the general-order kinetic model, because this was the best kinetic model to describe the kinetic experiments. By analyzing these values in Table 3, it could be inferred that the kinetics of adsorption of DCF is faster than that of NM. The $t_{1/2}$ values of the NM adsorption onto 1(500-15-0.5) are 38.8-fold higher than the values obtained for DCF. With the aid of Marvin Sketch 16.3.14.0 software, the polar surface area of DCF and NM was calculated. These values are 52.16 $A^2$ and 104.12 $A^2$ for DCF and NM, respectively. The bigger the polar surface area of the pharmaceutical, the higher the area of this molecule that interacts with the water. Since the adsorption of an organic molecule onto an active surface of carbon involves dehydration of the organic molecule before it can be adsorbed on the solid surface, the pharmaceutical which interacts more extensively with the solvent will possess a higher energy barrier to be surpassed so as to release the water to the bulk of the solution, and the adsorption of the adsorbate takes place on the adsorbent surface. Therefore, the difference in polar surface area of the pharmaceuticals explains why the kinetic of adsorption of DCF onto 1-(500-15-0.5) is faster than that of NM.

Also, the $t_{0.95}$ was used to calculate the time for the adsorbate to achieve the equilibrium on the adsorbent surface. Based on these values it was observed that the equilibrium for DCF was obtained after 0.2431 h (14.59 min) and for NM the equilibrium was attained after 3.429 h (205.7 min). For the remaining experiments, the time of contact between the adsorbent and adsorbate was fixed at 30 min for DCF and 4 h for NM, in order to guarantee that in these times of contact the equilibrium was attained.

**5. Equilibrium Studies and Maximum Adsorption Capacity**

Adsorption isotherms describe the relationship between the amount of adsorbate adsorbed by the adsorbent ($q_e$) and the adsorbate concentration remaining in solution after the system attains equilibrium ($C_e$) at a constant temperature. The adsorption parameters of the equilibrium models provide some insights into the adsorption mechanism, surface properties and affinity of the adsorbent for the adsorbate. In this work the Langmuir, Freundlich and Sips isotherm models were tested. The isotherms of adsorption were measured at 25°, 35° and 45 °C with DCF and NM onto 1(500-15-0.5), 6(650-37-1.0) and 9(800-15-1.5) ACs samples. These samples were chosen because they were pyrolyzed at three different pyrolysis temperatures and, taking out 500-15-0, they presented the lowest $S_{BET}$ value (9(800-15-1.5); 328.0 $m^2$ $g^{-1}$), the highest $S_{BET}$ value (1(500-15-0.5); 679 $m^2$ $g^{-1}$) and the most intermediate $S_{BET}$ value (6(650-37-1.0); 503.7 $m^2$ $g^{-1}$), as well as presented different uptake values for DCF and NM.

Table 4 and Supplementary Fig. 4(a)-(f) show the adsorption isotherm parameters (at 25°, 35° and 45 °C) and their curves (at 25 °C) of DCF and NM adsorbed onto 1(500-15-0.5), 6(650-37-1.0) and 9(800-15-1.5) ACs samples. Considering the SD values, the Sips model best described adsorption equilibrium data of both compounds DCF and NM on the three samples. The values of SD of the Langmuir model ranged from 3.741 to 4.434 for DCF and 3.137 to 8.283 for NM, while the Freundlich model ranges were 7.642 to 29.32 for DCF and 3.592 to 9.114 for NM. For Sips model the SD values ranged between 1.426 to 2.638 for DCF and 1.907 to 2.677 for NM.

Based on the lowest SD values, the best isotherm model fitted was the Sips for all sample adsorbents, (see Table 4), which means that the $q_e$ values fitted by the isotherm model were closest to the $q_e$ values measured experimentally.

The Sips isotherm model [41] is a combination of the Langmuir and Freundlich isotherm models; therefore, the monolayer assumption of Langmuir model is discarded and the infinite adsorption assumption that originates from the Freundlich model is not considered. The Sips model predicts that the active sites of the adsorbent cannot present the same energy. Therefore, the adsorbent may present active sites preferred by the adsorbate molecules for occupation [41]; however, saturation of the active sites should also occur unlike in the Freundlich isotherm model. Taking into account that the adsorbent used in this study has different functional groups as shown by the FTIR spectrum (see Fig. 4), that the adsorbent material presents some micropores and mesopores (see Fig. 1), it is expected that the active sites of the adsorbent will not possess the same energy—this fact is supported by the Sips isotherm model.

**Table 4. Isotherm parameters for DCF and NM adsorption on 1(500-15-1.5), 6(800-15-1.5) and 9(650-37-1.0) samples. Conditions: contact time of 90 min; pH of 7.0 and 10.0, respectively, and adsorbent mass of 30.0 mg for DCF and NM**

| | 1 (500-15-0.5) | | | 6 (800-15-1.5) | | | 9 (650-37-1.0) | | |
|---|---|---|---|---|---|---|---|---|---|
| | 25 °C | 35 °C | 45 °C | 25 °C | 35 °C | 45 °C | 25 °C | 35 °C | 45 °C |
| **DICLOFENAC** | | | | | | | | | |
| **Langmuir** | | | | | | | | | |
| $Q_{max}$ (mg $g^{-1}$) | 155.3 | 145.8 | 147.2 | 90.61 | 84.14 | 91.51 | 146.4 | 138.6 | 133.2 |
| $K_L$ (L $mg^{-1}$) | 0.3125 | 0.3014 | 0.3036 | 0.2102 | 0.1867 | 0.1914 | 0.3426 | 0.3621 | 0.3388 |
| $R^2_{adj}$ | 0.9891 | 0.9875 | 0.9802 | 0.9843 | 0.9788 | 0.8842 | 0.9914 | 0.9899 | 0.9885 |
| SD (mg $g^{-1}$) | 3.741 | 3.322 | 3.854 | 2.865 | 2.722 | 23.34 | 4.434 | 4.812 | 5.192 |
| **Freudlich** | | | | | | | | | |
| $K_F$ (mg $g^{-1}$ (mg $L^{-1})^{-1/nF}$) | 63.11 | 61.75 | 57.98 | 19.51 | 18.79 | 18.12 | 47.44 | 46.89 | 46.16 |
| $n_F$ | 6.081 | 6.112 | 5.845 | 6.317 | 6.115 | 6.004 | 7.869 | 7.524 | 7.301 |
| $R^2_{adj}$ | 0.9577 | 0.9502 | 0.9453 | 0.9690 | 0.9704 | 0.9771 | 0.9729 | 0.9701 | 0.9693 |
| SD (mg $g^{-1}$) | 7.642 | 7.985 | 8.251 | 29.32 | 28.02 | 27.95 | 14.53 | 14.87 | 15.64 |
| **Sips** | | | | | | | | | |
| $Q_{max}$ (mg $g^{-1}$) | 157.4 | 146.2 | 150.1 | 91.42 | 86.73 | 90.26 | 148.0 | 142.1 | 146.7 |
| $K_s$ (L $mg^{-1}$) | 0.1298 | 0.1423 | 0.1298 | 0.1972 | 0.2195 | 0.2014 | 0.1477 | 0.1984 | 0.1865 |
| $n_s$ | 0.6898 | 0.5964 | 0.6898 | 0.5928 | 0.5766 | 0.5687 | 0.6812 | 0.6632 | 0.6539 |
| $R^2_{adj}$ | 0.9967 | 0.9911 | 0.9905 | 0.9913 | 0.9875 | 0.9887 | 0.9997 | 0.9991 | 0.9984 |
| SD (mg $g^{-1}$) | 1.868 | 2.351 | 2.532 | 1.426 | 1.726 | 1.701 | 2.638 | 2.655 | 2.701 |
| **NIMESULIDE** | | | | | | | | | |
| **Langmuir** | | | | | | | | | |
| $Q_{max}$ (mg $g^{-1}$) | 58.33 | 51.76 | 56.45 | 39.73 | 35.98 | 38.36 | 42.44 | 38.41 | 40.43 |
| $K_L$ (L $mg^{-1}$) | 0.3902 | 0.3766 | 0.3863 | 0.2104 | 0.2061 | 0.2133 | 0.3682 | 0.3784 | 0.3555 |
| $R^2_{adj}$ | 0.8715 | 0.8725 | 0.8862 | 0.9584 | 0.9665 | 0.9678 | 0.9658 | 0.9698 | 0.9688 |
| SD (mg $g^{-1}$) | 8.283 | 8.288 | 8.136 | 3.183 | 3.377 | 3.344 | 3.137 | 3.465 | 3.348 |
| **Freudlich** | | | | | | | | | |
| $K_F$ (mg $g^{-1}$ (mg $L^{-1})^{-1/nF}$) | 24.69 | 23.22 | 22.78 | 13.46 | 13.02 | 12.78 | 21.24 | 19.84 | 18.13 |
| $n_F$ | 5.975 | 5.862 | 5.803 | 4.932 | 4.545 | 4.234 | 5.993 | 5.745 | 5.454 |
| $R^2_{adj}$ | 0.9442 | 0.9521 | 0.9455 | 0.9462 | 0.9412 | 0.9302 | 0.9729 | 0.9735 | 0.9701 |
| SD (mg $g^{-1}$) | 9.114 | 9.215 | 9.199 | 3.592 | 3.662 | 3.971 | 4.225 | 4.211 | 4.228 |
| **Sips** | | | | | | | | | |
| $Q_{max}$ (mg $g^{-1}$) | 66.45 | 64.82 | 65.88 | 46.35 | 42.75 | 45.95 | 43.01 | 40.83 | 42.24 |
| $K_s$ (L $mg^{-1}$) | 0.2624 | 0.2425 | 0.2415 | 0.1931 | 0.1925 | 0.2015 | 0.1475 | 0.1445 | 0.1483 |
| $N_s$ | 1.752 | 1.525 | 1.443 | 0.5631 | 0.5421 | 0.5126 | 0.6815 | 0.6532 | 0.5432 |
| $R^2_{adj}$ | 0.9925 | 0.9911 | 0.9986 | 0.9851 | 0.9834 | 0.9821 | 0.9871 | 0.9866 | 0.9805 |
| SD (mg $g^{-1}$) | 2.095 | 2.125 | 2.221 | 1.907 | 1.998 | 1.882 | 2.677 | 2.845 | 2.994 |

The effect of temperature on the percentage of removal of DCF and NM by ACs was also evaluated in this work and its results are shown in Table 4. It was observed that $Q_{max}$ and K of Langmuir and Sips did not follow a regular pattern, a fact that precludes the determination of the thermodynamic parameters as early reported [2,20,21, 26].

To compare the efficiency of the sludge-activated carbons studied, Table 5 shows a comparison between the maximum adsorption capacities between the ACs studied and various other adsorbents reported in the literature [2,16,18,49,50,52-56]. As can be seen in Table 5, the adsorbent material proposed in this current work presents very good adsorption capacities when compared with other adsorbents reported in the literature. For DCF out of a total of 13 adsorbents the 1(500-15-0.5) sludge activated carbon presented sorption capacity higher than 11; and for NM, out of a total of 6 adsorbents, the 1-(500-15-0.5) adsorbent presented sorption capacity higher than 5.

Fig. 7 shows the sorption capacities obtained with an initial concentration of 1,000 mg $L^{-1}$ of DCF and NM ($q_e^{1000}$) for all produced activated carbons. From Fig. 7 it is possible to see that the sample not treated chemically 10(500-15-0) showed the lowest $q_e^{1000}$ for both compounds DCF and NM, while sample 1(500-15-0.5) presented the highest $q_e^{1000}$ value. This behavior corresponds to the magnitude of $S_{BET}$ values (Table 2), which may help to explain the $q_e^{1000}$ variations. As can be seen from Table 2 and Fig. 5, generally the $q_e^{1000}$ value is higher on AC with higher $S_{BET}$. This suggests that $S_{BET}$ influenced the uptake of both adsorbates significantly.

Fig. 7 demonstrates that $Q_{max}$ of DCF is much higher than NM.

**Table 5. Comparison of adsorption capacities of different adsorbents for DCF and NM**

| | Adsorption capacity (mg $g^{-1}$) | | |
|---|---|---|---|
| Adsorbent | DCF | NM | Reference |
| Activated carbon from cocoa shell | 63.47 | 74.81 | [2] |
| PAC | 372.0 | - | [16] |
| PAC | 233.9 | - | [18] |
| Modified chitosan | 9.33 | - | [49] |
| Functionalized silica | 35.59 | - | [50] |
| Composite adsorbent | 27.18 | 14.55 | [52] |
| Hybrid adsorbent | 41.43 | 26.12 | [52] |
| Sludge activated carbon | 16.27 | 9.438 | [52] |
| Multi-walled carbon nanotubes | 8.640 | - | [53] |
| Carbon xerogels | 80.00 | - | [54] |
| PAC | 40.55 | - | [55] |
| Mesoporous silica (SBA-15) | 34.18 | - | [56] |
| Silica aerogel | - | 14.18 | [56] |
| 1 (500-15-0.5) sludge activated carbon | 157.4 | 66.45 | This work |

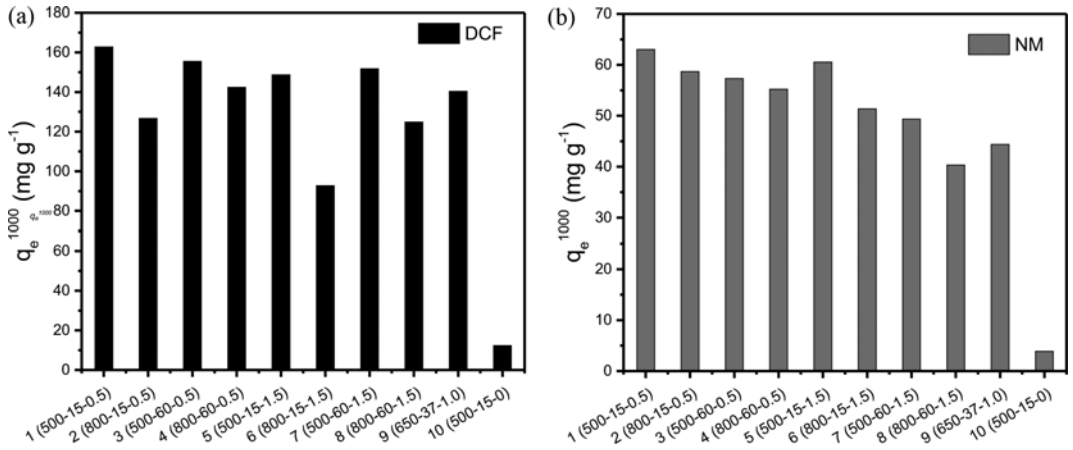


**Fig. 7. Adsorption capacity of 1,000 mg $L^{-1}$ ($q_e^{1000}$) of DCF and NM onto sludge based activated carbons at 25 °C.**

Also the rate of adsorption of DCF was faster than that of NM according to $t_{1/2}$ (see Table 3). The higher affinity of sludge activated carbons by DCF rather than NM could be linked to their differences in chemical properties. The van der Waals surface area of DCF and NM was 359.64 $A^2$ and 406.46 $A^2$, respectively (see Table 1), while the polar surface area of DCF and NM was 52.16 $A^2$ and 104.12 $A^2$, respectively (see Table 1). Performing the division of polar surface area by van der Waals surface area and multiplying by 100, the percentage of polar area in relation to the total area of DCF is 14.50% and for NM is 25.62%. Considering that the activated carbons are hydrophobic, as can be seen in Fig. 3, it is expected that DCF would have higher affinity of the hydrophobic surface of the activated carbon when compared with NM.

**6. Adsorption Mechanism**

Based on the combined data of characterization of materials as well as the kinetic and equilibrium studies, it is possible to suggest mechanisms for adsorption of DCF and NM onto AC adsorbents. The adsorption process involves physical interactions such as van der Waals interactions, hydrogen bonding and $\pi$-$\pi$ interactions of the aromatic ring of the adsorbent with the aromatic rings of the pharmaceuticals. The aromatic rings of pharmaceuticals interact with the phenyl, OH, C=O and COOH groups of the ACs through $\pi$-$\pi$ interactions as shown in Fig. 8.

## CONCLUSION

Activated carbons have been prepared using sewage sludge as starting material and a conventional furnace pyrolysis for heat treatment. The powdered sewage sludge and $ZnCl_2$ were mixed in different proportions at room temperature. The mixture was heated at three different temperatures, 500°, 650° and 800 °C, under inert conditions. The carbonized materials were treated with a 6 mol $L^{-1}$ HCl and refluxed for 3 h to obtain chemically activated ACs. The acidification process leached the inorganics from the carbonaceous matrix, which was confirmed by BET surface area and SEM techniques. According to water and n-heptane adsorption, the samples of ACs were hydrophobic. The sample 1(500-15-0.5) was identified to be the best adsorbent for the removal of DCF and

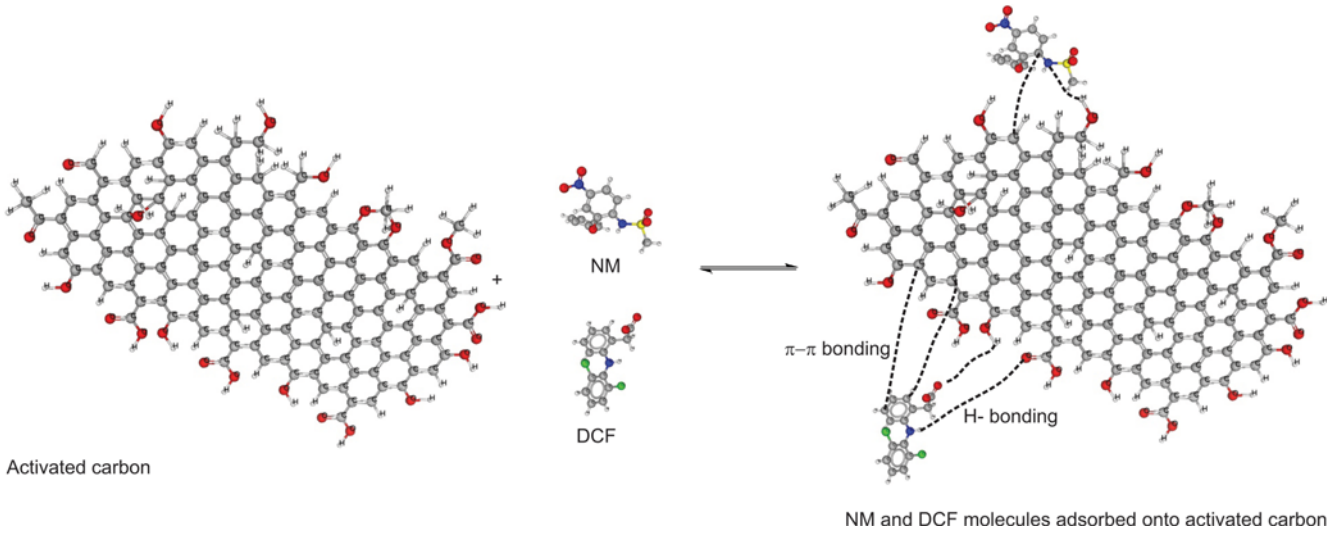


**Fig. 8. Adsorption mechanism of DCF and NM onto AC.**

NM from aqueous solutions. Adsorption capacity of the ACs produced within this work is among the highest of many works found in literature. At 25 °C, it was observed that the equilibrium for DCF was obtained after 0.2431 h (14.59 min) and for NM the equilibrium was attained after 3.429 h (205.7 min). The general-order kinetic model best described the adsorption process, because the order of adsorption was experimentally measured instead of being restricted by a given model. Sips isotherm model gave the best fit of isothermal data, showing that an adsorption process should occur in multiple sites of the activated carbon. The maximum amounts ($Q_{max}$) of DCF and NM adsorbed were 157.4 and 66.45 mg $g^{-1}$ for 1(500-15-0.5), respectively.

## ACKNOWLEDGEMENTS

The authors thank the National Council for Scientific and Technological Development (CNPq, Brazil), the Coordination of Improvement of Higher Education Personnel (CAPES, Brazil), and the German Academic Exchange Service (DAAD, Germany) for financial support, fellowships, grants and technical support. We thank Chemaxon for giving an academic research license for the Marvin Sketch software, Version 16.3.14.0, (http://www.chemaxon.com), 2016 used for the pharmaceuticals physical-chemical properties.

## SUPPORTING INFORMATION

Additional information as noted in the text. This information is available via the Internet at http://www.springer.com/chemistry/journal/11814.

## REFERENCES

1. S. Rovani, M. T. Censi, S. L. Pedrotti-Jr., E. C. Lima, R. Cataluña and A. N. Fernandes, *J. Hazard. Mater.*, **271**, 311 (2014).
2. C. Saucier, M. A. Adebayo, E. C. Lima, R. Cataluna, P. S. Thuea, P. D. T. Lizie, P.-M. J. Rosero, F. M. Machado, F. A. Pavan and G. L. Dotto, *J. Hazard. Mater.*, **289**, 18 (2015).
3. R. Gothwal and T. Shashidhar, *Clean - Soil Air Water*, **43**, 479 (2015).
4. L. Prieto-Rodríguez, I. Oller, N. Klamerth, A. Agüera, E. M. Rodríguez and S. Malato, *Water Res.*, **47**, 1521 (2013).
5. N. Bolong, A. F. Ismail, M. R. Salim and T. Matsuura, *Desalination*, **239**, 229 (2009).
6. H. J. Lee, E. Lee, S. H. Yoon, H. R. Chang, K. Kim and J. H. Kwon, *Chemosphere*, **87**, 969 (2012).
7. Y. Li, G. Zhu, W. J. Ng and S. K. Tan, *Sci. Total Environ.*, **468-469**, 908 (2014).
8. N. Han, T. Taro, U. Thi and T. Ta, *Clean - Soil Air Water*, **42**, 267 (2014).
9. E. Geiger, R. Hornek-Gausterer and M. T. Saçan, *Ecotoxicol. Environ. Saf.*, **129**, 189 (2016).
10. R. Feito, Y. Valcárcel and M. Catalá, *Ecotoxicology*, **21**, 289 (2012).
11. M. Boonsaner and D. W. Hawker, *Chemosphere*, **122**, 176 (2015).
12. C. Sheng, A. G. A. Nnann, Y. Liu and J. D. Vargo, *Sci. Total Environ.*, **550**, 1075 (2016).
13. J. B. Parsa, T. M. Panah and F. N. Chianeh, *Korean J. Chem. Eng.*, **33**, 893 (2016).
14. W. Gebhardt and H. F. Schroder, *J. Chromatogr. A*, **1160**, 34 (2007).
15. S. Suarez, J. M. Lema and F. Omil, *Bioresour. Technol.*, **100**, 2138 (2009).
16. C. Jung, L. K. Boateng, J. R. V. Flora, J. Oh, M. C. Braswell, A. Son and Y. Yoon, *Chem. Eng. J.*, **264**, 1 (2015).
17. L. R. Rad, M. Irani and R. Barzegar, *Korean J. Chem. Eng.*, **32**, 1606 (2015).
18. J. L. Sotelo, G. Ovejero, A. Rodríguez, S. Álvarez, J. Galán and J. García, *Chem. Eng. J.*, **240**, 443 (2014).
19. G. L. Dotto, E. C. Lima and L. A. A. Pinto, *Bioresour. Technol.*, **103**, 123 (2012).
20. L. D. T. Prola, E. Acayanka, E. C. Lima, C. S. Umpierres, J. C. P. Vaghetti, W. O. Santos, S. Laminsi and P. T. Njifon, *Ind. Crop Prod.*, **46**, 328 (2013).
21. D. C. dos Santos, M. A. Adebayo, S. F. P. Pereira, L. D. T. Prola, R. Cataluña, E. C. Lima, C. Saucier, C. R. Gally and F. M. Machado,

*Korean J. Chem. Eng.*, **31**, 1470 (2014).
22. S. Sadaf and H. N. Bhatti, *Clean Technol. Environ. Policy.*, **16**, 527 (2014).
23. G. S. dos Reis, M. Wilhelm, T. C. A. Silva, K. Rezwan, C. H. Sampaio, E. C. Lima and S. M. A. G. U. Souza, *Appl. Therm. Eng.*, **93**, 590 (2016).
24. T. Calvete, E. C. Lima, N. F. Cardoso, J. C. P. Vaghetti, S. L. P. Dias and F. A. Pavan, *J. Environ. Manage.*, **91**, 1695 (2010).
25. H. Marsh and F. R. Reinoso, Activated Carbon. Elsevier, Amsterdam (2006).
26. M. C. Ribas, M. A. Adebayo, L. D. T. Prola, E. C. Lima, R. Cataluña, L. A. Feris, M. J. Puchana, F. M. Machado, F. A. Pavan and T. Calvete, *Chem. Eng. J.*, **248**, 315 (2014).
27. S. Brunauer, P. H. Emmett and E. Teller, *J. Am. Chem. Soc.*, **60**, 309 (1938).
28. E. P. Barrett, I. G. Joyner and P. P. Halend, *J. Am. Chem. Soc.*, **73**, 373 (1951).
29. L. Leng, X. Yuana, H. Huang, J. Shao, H. Wang, X. Chen and G. Zeng, *Appl. Surf. Sci.*, **346**, 223 (2015).
30. A. V. Maldhure and J. D. Ekhe, *Chem. Eng. J.*, **168**, 1103 (2011).
31. T. Calvete, E. C. Lima, N. F. Cardoso, S. L. P. Dias and E. S. Ribeiro, *Clean: Air, Soil, Water,* **38**, 521 (2010).
32. E. C. Lima, F. Barbosa-Jr., F. J. Krug and U. Guaita, *J. Anal. Atom. Spectrom.*, **14**, 1601 (1999).
33. E. C. Lima, F. Barbosa-Jr., F. J. Krug and A. Tavares, *Talanta*, **57**, 177 (2002).
34. E. C. Lima, F. J. Krug, J. A. Nóbrega and A. R. A. Nogueira, *Talanta*, **47**, 613 (1998).
35. E. C. Lima, P. G. Fenga, J. R. Romero and W. F. de Giovani, *Polyhedron*, **17**, 313 (1998).
36. C. Saucier, M. A. Adebayo, E. C. Lima, L. D. T. Prola, P. S. Thue, C. S. Umpierres, M. J. Puchana-Rosero and F. M. Machado, *Clean.*, **43**, 1389 (2015).
37. W. S. Alencar, E. C. Lima, B. Royer, B. D. dos Santos, T. Calvete, E. A. da Silva and C. N. Alves, *Sep. Sci. Technol.*, **47**, 513 (2012).
38. E. C. Lima, M. A. Adebayo and F. M Machado, *Chapter 3- Kinetic and Equilibrium Models of Adsorption in Carbon Nanomaterials as Adsorbents for Environmental and Biological Applications*, C. P. Bergmann and F. M. Machado, Eds., Springer (2015).
39. I. Langmuir, *J. Am. Chem. Soc.*, **40**, 1361 (1918).
40. H. Freundlich, *Phys. Chem. Soc.*, **40**, 1361 (1906).
41. R. Sips, *J. Chem. Phys.*, **16**, 490 (1948).
42. P. B. Balbuenat and K. E. Gubbins, *Langmuir*, **9**, 1801 (1993).
43. T. Prenzel, T. L. M. Guedes, F. Schluter, M. Wilhelm and K. Rezwan, *Sep. Purif. Technol.*, **129**, 80 (2014).
44. S. W. Nam, D. J. Choi, S. K. Kim, N. Her and K. D. Zoh, *J. Hazard. Mater.*, **270**, 144 (2014).
45. S. Biniak, G. Szymanski, J. Siedlewski and A. Swiatkowski, *Carbon*, **35**, 1799 (1997).
46. Y. Otake and R. G. Jenkins, *Carbon*, **31**, 109 (1993).
47. K. M. Smith, G. D. Fowler, S. Pullket and N. D. J. Graham, *Water Res.*, **43**, 2569 (2009).
48. G. B. Gasco, C. G. Guerrero, F. Mendez and A. M. Lazaro, *J. Anal. Appl. Pyrol.*, **74**, 413 (2005).
49. K. A. A. Pereira, L. R. Osório, M. P. Silva, K. S. Sousa and E. C. S. Filho, *Mat. Res.*, **17**, 1516 (2014).
50. N. Suriyanon, P. Punyapalakul and C. Ngamcharussrivichai, *Chem. Eng. J.*, **214**, 208 (2013).
51. T. X. Bui and H. Choi, *J. Hazard. Mater.*, **168**, 602 (2009).
52. G. S. dos Reis, C. H. Sampaio, E. C. Lima and M. Wilhelm, *Colloids Surf. A Physicochem. Eng. Asp.*, **497**, 304 (2016).
53. X. Hu and Z. Cheng, *Chin. J. Chem. Eng.*, **23**, 1551 (2015).
54. S. Álvarez, R. S. Ribeiro, H. T. Gomes, J. L. Sotelo and J. García, *Chem. Eng. Res. Des.*, **95**, 229 (2015).
55. C. M. Dai, S. U. Geissen, Y. L. Zhang, Y. J. Zhang and X. F. Zhou, *Environ. Pollut.*, **159**, 1660 (2011).
56. G. Caputo, M. Scognamiglio and I. De Marco, *Chem. Eng. Res. Des.*, **90**, 1082 (2012).

# Supporting Information

# Activated carbon from sewage sludge for removal of sodium diclofenac and nimesulide from aqueous solutions

**Glaydson Simões dos Reis[*,**,†], Mohammad Khalid Bin Mahbub[**], Michaela Wilhelm[**], Eder Claudio Lima[***], Carlos Hoffmann Sampaio[*], Caroline Saucier[***], and Silvio Luis Pereira Dias[***]**

*Department of Metallurgical Engineering, Federal University of Rio Grande do Sul (UFRGS), Av. Bento Gonçalves 9500, Porto Alegre, RS, Brazil
**University of Bremen, Advanced Ceramics, Am Biologischen Garten 2, IW3, 28359 Bremen, Germany
***Institute of Chemistry, Federal University of Rio Grande do Sul (UFRGS), Av. Bento Gonçalves 9500, Postal Box 15003, ZIP 91501-970, Porto Alegre, RS, Brazil
(*Received 5 February 2016 • accepted 2 July 2016*)

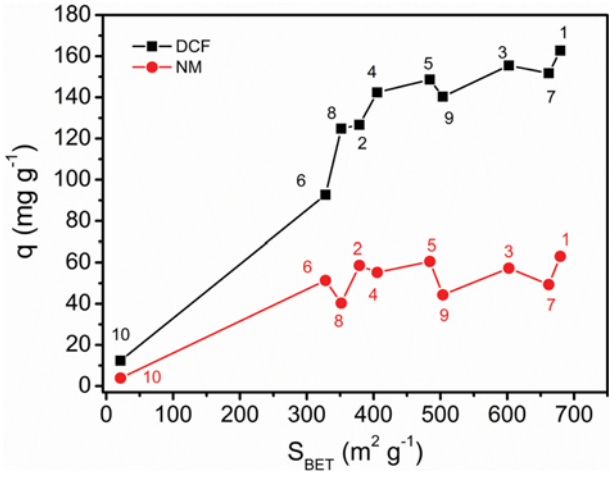


**Fig. S1. Adsorption isotherm models fitting in the adsorption of diclofenac and nimesulide by hybrid materials.**

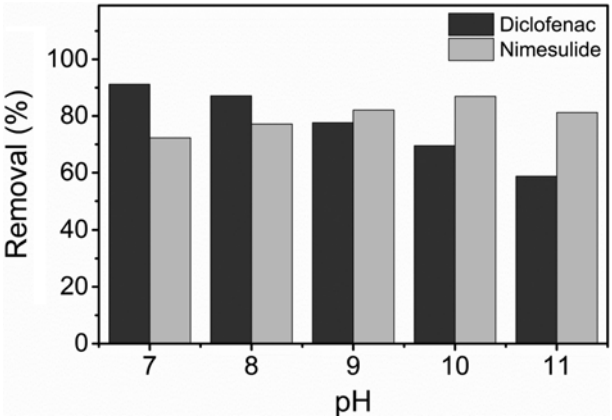


**Fig. S2. Dependence of pH on the sorption capacity of DCF and NM pharmaceuticals on 1(500-15-0.5). Conditions: temperature, 25 °C; adsorbent mass, 20.0 mg; adsorbent 25 °C pharmaceutical concentration, 50.0 mg L.**

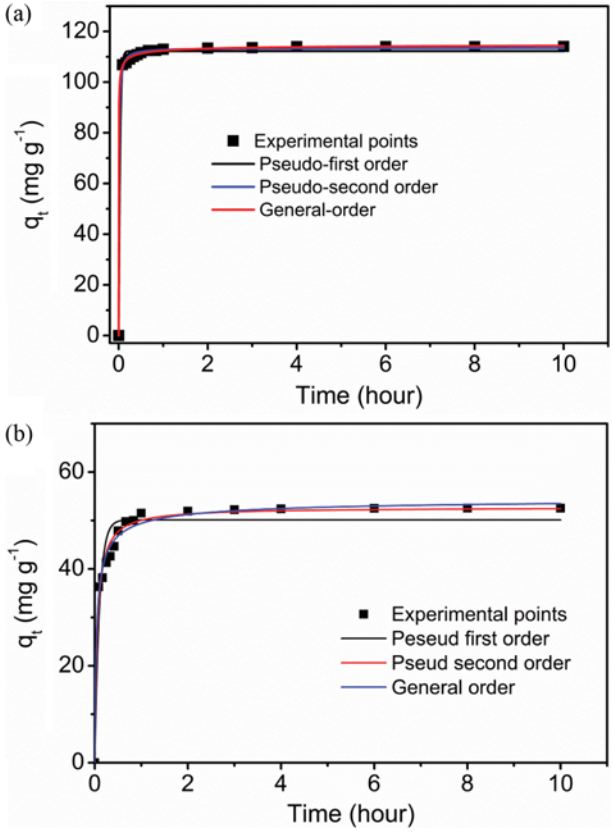


**Fig. S3. Adsorption kinetic models fitting in the adsorption of diclofenac and nimesulide onto 1(500-15-0.5) sample.**

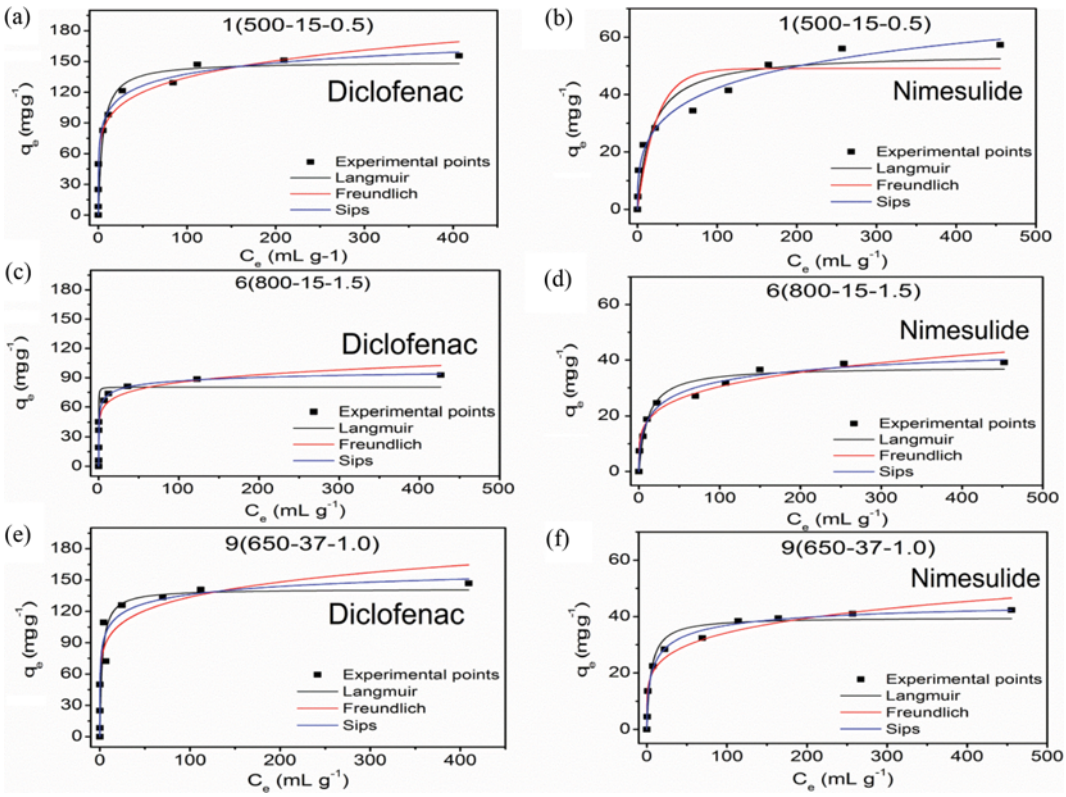


**Fig. S4. Adsorption isotherm models fitting in the adsorption of diclofenac and nimesulide by hybrid materials.**